

## Characterization of basal nitric oxide production in living cells

Manuel O. López-Figueroa <sup>a,\*</sup>, Claudio Caamaño <sup>a</sup>, Raquel Marin <sup>b</sup>, Borja Guerra <sup>b</sup>,  
Rafael Alonso <sup>b</sup>, M. Inés Morano <sup>a</sup>, Huda Akil <sup>a</sup>, Stanley J. Watson <sup>a</sup>

<sup>a</sup> *Mental Health Research Institute, University of Michigan, 205 Zina Pitcher Place, Ann Arbor, MI 48109, USA*

<sup>b</sup> *Department of Physiology, School of Medicine, University of La Laguna, Tenerife, Spain*

Received 16 April 2001; received in revised form 12 June 2001; accepted 3 July 2001

### Abstract

Nitric oxide (NO) is an important modulator of immune, endocrine and neuronal functions; however, measuring physiological levels of NO in cell cultures is generally difficult because of the lack of suitable methodologies. We have selected three cell lines from different origins: the neuroblastoma-derived Neuro2A (N2A), the cholinergic SN56 and the non-neuronal COS-1. We first demonstrated the presence of NADPH-diaphoretic activity, a potential marker of the NO-synthesizing (NOS) enzyme. By immunocytochemistry, using specific antibodies for each NOS subtype, we observed that subtype I was present in all cell lines and that subtype II was present in COS-1 and N2A cell lines. The presence of these NOS subtypes was further verified by Western blot analysis. Control cells treated with DAF-2 DA exhibited significant fluorescent levels corresponding to basal NO production. The subcellular distribution of the synthesizing enzyme was consistent with the NO-fluorescence signal; whereas, fixation affected the subcellular pattern of NO fluorescence signal. Addition of NOS inhibitors or NO scavengers to the incubation medium reduced the intensity of the NO fluorescence signal in a concentration-dependent manner. Conversely, increasing concentrations of a NO donor, or incident light, increased the fluorescence intensity. Our observation of NO production and distribution using the DAF-2 method has a direct impact on studies using these cell lines. © 2001 Elsevier Science B.V. All rights reserved.

*Keywords:* Nitric oxide synthase; Diaminofluorescein; COS-1; N2A; SN56

### 1. Introduction

Nitric oxide synthase (NOS) is an enzyme that uses L-arginine as a substrate, producing the free radical NO and L-citrulline as coproducts. Three subtypes of NOS have been described in detail [1,2]. NOS subtypes I, II and III are also commonly

known as neuronal, inducible and endothelial, respectively. Under basal conditions NOS subtypes I and III produce small amounts of NO. Activation of receptors leads to either direct or G-protein-mediated increase in intracellular Ca<sup>2+</sup>. The elevated Ca<sup>2+</sup> levels activate NOS-I and III, resulting in increased production of NO. Then, NO activates soluble guanylate cyclase, leading to production of cGMP, which plays a role in several physiological functions. In contrast, the transcriptional activation of NOS-II produces large amounts of NO, independent of Ca<sup>2+</sup> concentrations. The NO produced by this subtype

\* Corresponding author. Fax: +1-734-647-4130.

E-mail address: molff@umich.edu (M.O. López-Figueroa).

reacts with superoxide to produce peroxynitrite, a highly cytotoxic molecule. The roles played by NO are myriad, such as regulation of neurotransmitter secretion, neurotoxicity, modulation of the immune response or regulation of blood flow.

NO is an atypical biomolecule with an ultra-short half-life and highly diffusible upon formation [3]. Due to its high reactivity, most of the methods currently available for detecting the *in situ* production of NO in cells are indirect. Some techniques, like *in situ* hybridization, allow a semiquantitative measurement of transcriptional changes in NOS mRNAs. Alternatively, immunocytochemistry allows the determination of the cellular and sub-cellular localization of each of the NOS subtypes at the protein level. In addition, the NADPH-diaphorase histochemical reaction has been broadly used as a potential marker of NO-synthesizing enzymes [4,5]. Other direct methods, such as NO-electrodes, or indirect ones, such as the Griess or the EPR spin trapping method, are available to measure NO or NO derivatives such as nitrites and nitrates that are released in the media. However, these last methods lack the anatomical resolution provided by the previously mentioned ones (for review, see [6]). A simple and reliable method for evaluating the *in vivo* production of NO using the compound DAF-2 DA has been recently developed [7]. DAF-2 DA penetrates the cell membrane where it is hydrolyzed by cytosolic esterases. In the presence of oxygen, DAF-2 DA or DAF-2 traps NO to produce a green-fluorescence signal, triazolofluorescein. The DAF-2 has low detection limits (2–5 nM) and broad concentration response range, which allows semiquantitative analysis.

A diversity of cell types are capable of producing the different types of NOS and regulating their expression in tissues. In particular, NOS-II seems to be expressed in a variety of cells following induction by immunologic or inflammatory stimuli [8,9]. Cell cultures are broadly used as a model to investigate mechanisms of signal transduction, regulation of gene expression, cell differentiation and death. Therefore, given the multiple physiological and pathological effects of NO in most of the cell functions [8,10], the intracellular NO levels should be considered as a potential variable affecting signal-transduction path-

ways. Moreover, the endogenous production of the free radical in cell lines should facilitate further mechanistic studies of regulation of NO production. Thus, the aim of this study was to establish the presence of NO, and the subtypes of NOS responsible for its production in commonly used cell lines. Two murine neuronal cell lines, the neuroblastoma N2A and the cholinergic SN56, and a transformed monkey kidney cell line, COS-1, were selected. The basal production and the regulation of NO production in these cell lines was determined using the DAF-2 DA method upon treatment with specific NOS inhibitors, NO scavengers, and a NO donor. In addition, we evaluated the effect of incident light and fixation on the pattern of NO production revealed by the DAF-2 DA method. The ability to detect NO *in vivo* in these cell lines adds a new reference point for monitoring this particular molecule and its interaction with other systems. This will help to provide a more comprehensive view of the role of NO in cellular signaling.

## 2. Materials and methods

### 2.1. Cell culture

COS-1 and N2A cells were obtained from the American Type Culture Collection (Rockville, MD), and SN56 cells were a gift from Dr. B. Wainer (Boston University School of Medicine, MA). Cells were maintained in Dulbecco's modified Eagle's medium (DMEM) (Life Technologies, Rockville, MD) devoid of phenol-red and supplemented with 10% fetal bovine serum (FBS) (Hyclone Labs, Logan, UT) at 37°C with 5% CO<sub>2</sub>. For Western immunoblotting studies, the cells were plated on 10-cm tissue culture dishes at 1 × 10<sup>6</sup> cells/dish. For all other experiments, the cells were plated on 8-well slides (Nunc, Rochester, NY) precoated with polylysine to yield a density of 3.5 × 10<sup>3</sup> cells/well. All cultures were used 16 h after plating. In one experiment with SN56 cells, nerve growth factor (NGF) (Life Technologies) was added to the media at a 10 ng/ml concentration the day before processing. For the drug treatment experiments, cultures were washed in fresh

DMEM with 10% FBS and incubated for 1 h in the same media with or without the appropriate concentration of drug.

### 2.2. 4,5-Diaminofluorescein diacetate (DAF-2 DA) detection system

For the detection of the NO production, cells were incubated in 10  $\mu$ M DAF-2 DA (Calbiochem, San Diego, CA) for 30 min at 37°C in a humidified incubator under an atmosphere with 5% CO<sub>2</sub>. This method has been previously described in detail [11]. For drug treatment experiments, cells were first incubated for 1 h in the DMEM containing the appropriate concentration of the drug. We used the NO scavenger, 2-phenyl-4,4,5,5-tetramethylimidazoline-1-oxyl-3-oxide (PTIO), the NOS inhibitors *N*-[3-(aminomethyl)benzyl]acetamide dihydrochloride (1400W) and *N*<sup>ω</sup>-propyl-L-arginine (NPA), all from Calbiochem, and the NO donor sodium nitroprusside from Fisher Scientific (S-350, Fair Lawn, NJ). Then the medium was discarded and the cells were incubated in the DAF-2 DA as previously described. For fixation, cells were incubated for 1 h in 0.2% glutaraldehyde and 4% paraformaldehyde (PA). Alternatively, fixation was performed in 2% PA or 4% PA alone. Control cells were incubated in the same media without any drug. As negative control, cells were incubated in media lacking DAF-2 DA. The cells were then washed in PBS and coverslipped using Aquamount as the mounting medium.

### 2.3. NADPH-diaphorase cytochemistry

The NADPH-d method was used as previously described by López-Figueroa and collaborators [12]. Briefly, cells were fixed in 2% paraformaldehyde (PA) in PBS for 10 min at room temperature (RT). Cells were then washed and incubated in a solution containing 1mM  $\beta$ -nicotinamide adenine dinucleotide phosphate ( $\beta$ -NADPH, Sigma, St. Louis, MO) and 0.1 mM nitro blue tetrazolium (NBT; Sigma) in phosphate-buffered saline (PBS, pH 7.4) for 1 h at 37°C. Cells were then washed, dehydrated and coverslipped. In order to colocalize NO production with NADPH-d activity, a subset of the cells were reacted

with DAF-2 DA prior to fixation (see below). Control experiments were performed by omitting  $\beta$ -NADPH.

### 2.4. Immunocytochemistry

After fixation in 2% PA for 10 min, cells were washed and incubated in an avidin and biotin blocking solution (Vector Labs, Burlingame, CA) for 10 min each, at RT. For NO colocalization, a subset of the cells was reacted with DAF-2 DA prior to fixation. Following incubation in 1% bovine serum albumin (BSA) (Sigma) and 0.3% Triton X-100 for 20 min at RT, cells were further incubated overnight at 4°C in the same BSA solution containing the corresponding anti NOS-I (diluted 1:3000, Euro-Diagnostica, Malmo, Sweden; diluted 1:1000, Transduction Laboratories, Lexington, KY), anti NOS-II (diluted 1:2500, Affinity Bioreagents, Golden, CO) and anti NOS-III (diluted 1:2500, Transduction Laboratories) polyclonal antibody. After three 5-min washes in PBS, cells were incubated in biotin-conjugated secondary antibody (diluted 1:1000, Vector Labs) for 1 h at RT. After washing as above, cells were incubated in rhodamine-conjugated avidin (diluted 1:1000 in PBS, Vector Labs) for 1 h at RT. For comparison, some cell cultures were developed using the DAB method as previously described [13]. The cells were then washed and coverslipped using Aquamount as mounting medium.

### 2.5. Western blots

Cells were harvested by scraping with a rubber policeman or trypsinized (0.25% in PBS) in the case of SN56 cells, and then washed three times with PBS. Cell pellets were resuspended in 500  $\mu$ l of the buffer TEDGM (20 mM sodium molybdate, 20 mM Tris-HCl, 1 mM EDTA, 5 mM dithiothreitol, 5  $\mu$ g/ml leupeptin, 0.5 mM PMSF, and 10% glycerol, pH 7.6), homogenized at 0°C by 20 strokes in a Dounce homogenizer, and centrifuged at 100 000  $\times$ g for 1 h at 2°C. Aliquots (20  $\mu$ g protein) of the resulting cytosolic fractions were electrophoresed in 8% sodium dodecyl sulfate-polyacrylamide slab gels [14]. For electroblotting, gels were equilibrated for 1 h at RT

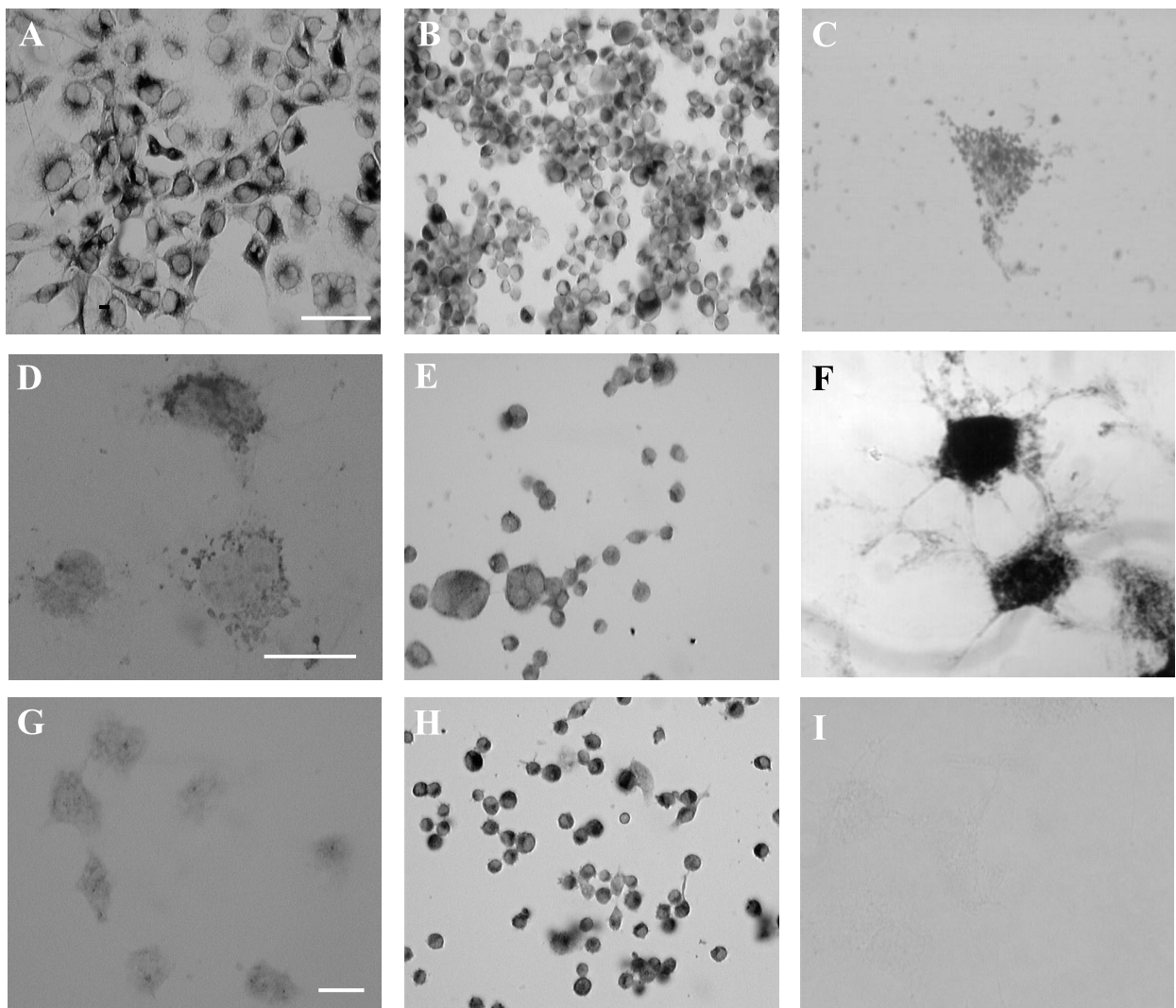


Fig. 1. Identification of NOS in COS-1 (A,D,G), N2A (B,E,H) and SN56 (C,F) cells. NADPH-diaphorase activity is present in the cytosol and the periphery of the nucleus of COS-1 (A), N2A (B) and SN56 (C). COS-1 (D,G), N2A (E,H) and SN56 (F,I) cells immunostained with a polyclonal antibody against NOS-I (D–F) and NOS-II (G,H). Control immunocytochemistry in the absence of the primary antibodies (I). Scale bars: A,B,H = 50  $\mu$ m; C–F,H,I = 25  $\mu$ m; G = 25  $\mu$ m.

in a transfer buffer consisting of 25 mM Tris, 192 mM glycine and 10% methanol, pH 8.5. Protein transfer onto Immobilon-P membranes (Millipore Corp., Bedford, MA) proceeded for 2 h at 200 V in ice bath. The efficiency of the process was assessed by the transfer of prestained molecular mass markers loaded in at least one lane of the gel. Membrane strips were eventually saved for staining (10 min) in 0.1% Coomassie blue, 10% methanol, and 5% acetic acid. The entire immunostaining procedure was performed at RT as follows. Blots were first washed three times in buffer A composed of TBS (20 mM

Tris-HCl, 150 mM NaCl, pH 7.6) and 0.1% Tween 20. Blots were subsequently blocked by incubation for 1 h in a solution of 10% nonfat dry milk, 0.5% Tween 20, and TBS. After washing three times in buffer A, blots were incubated for 1 h in a solution containing the primary rabbit polyclonal antibodies against NOS-I, -II and -III at a concentration of 1:10 000, 1:4000 and 1:4000, respectively, in buffer B (1% nonfat dry milk, 0.1% Tween 20, TBS). Blots were extensively washed three times for 15 min in buffer A and incubated for 1 h in a solution containing a 1:4000 dilution of horseradish peroxidase-

coupled second antibody (Amersham Pharmacia Biotech, Piscataway, NJ) in buffer B. After extensive washing as described above, blots were incubated with the Enhanced Chemi-Luminescence detection system according to the manufacturer's instructions (Amersham Pharmacia Biotech), and emitted light was detected by direct exposure to Hyperfilm-ECL film (Amersham Pharmacia Biotech).

### 2.6. Image analysis

Images of reacted cells were rapidly digitized with a Sony DXC-970MD video camera connected to a Leica DHR epifluorescence microscope. All of the images of each experiment were captured under constant exposure time, gain and offset. Images were further analyzed with the MCID image analysis system (Imaging, Ontario, Canada). The results are expressed as relative optical densities (ROD), which represent the mean optical density minus background, multiplied by the total target area. Background was calculated as the mean of all pixels with lowest optical density outside a cell multiplied by 3.5 times its standard deviation. Values are the result of the analysis of at least eight images per experimental condition, with at least 20 cells per experimental condition and image. Each condition was repeated at least three times.

### 2.7. Statistical analysis

The data are expressed as mean  $\pm$  S.E.M. Statistical analysis was made by one-way analysis of variance (ANOVA) followed by post hoc Dunnett's (vs. corresponding control) multiple comparison test. Values of  $P < 0.05$  were considered statistically significant.

## 3. Results

To determine the source of NO production, we visualized the presence of NOS by NADPH-diaphorase cytochemistry, and by immunocytochemistry using specific NOS antibodies. We further characterized the immunocytochemical findings by Western blots. Then, NO production was visualized and characterized using the DAF-2 DA system.

### 3.1. NADPH-diaphorase

NADPH-d cytochemistry is an indirect method for detecting NOS activity. We observed positive staining in all cell lines (Fig. 1A–C). The intensity of the staining was heterogeneous suggesting different levels of activity, as confirmed with the DAF-2 DA system (see below). The subcellular distribution of the NADPH-d staining was also heterogeneous and in most cases showed a punctate pattern. Nuclei were devoid of signal and were usually surrounded by an intense NADPH-d staining. Star-shaped COS-1 and SN56 cells presented positive fiber-like structures that were less evident in rounded N2A. All cells positive for NADPH-d were also positive for DAF-2 (data not shown). No staining was observed in control cells reacted without  $\beta$ -NADPH.

### 3.2. Immunocytochemistry

To identify the subtype of NOS responsible for the observed NO production, immunocytochemistry (Fig. 1) and Western blots (see below) were performed in cell extracts using specific antibodies against the three subtypes of NOS. As shown in Fig. 1D–H, the pattern of NOS I and II subcellular immunoreactivity was similar to that described above

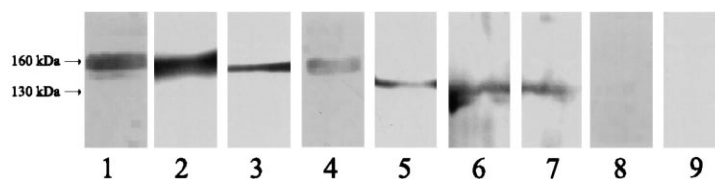


Fig. 2. Western blot analysis of NOS in COS-1, SN56 and N2A. Lanes: 1,5, positive controls for NOS-I and -II, respectively; 2,6, COS-1 extracts; 3,7, N2A extracts; 4,8, SN56 extracts. Lanes 1–4 were reacted with anti-NOS-I antibody and lanes 5–8 with NOS-II. None of the extracts exhibited immunoreactivity towards NOS-III antibody and, for illustration, only the negative result obtained with COS-1 cells is shown in lane 9. Molecular masses were 160, 130 and 135 kDa for NOS-I, -II and -III, respectively.

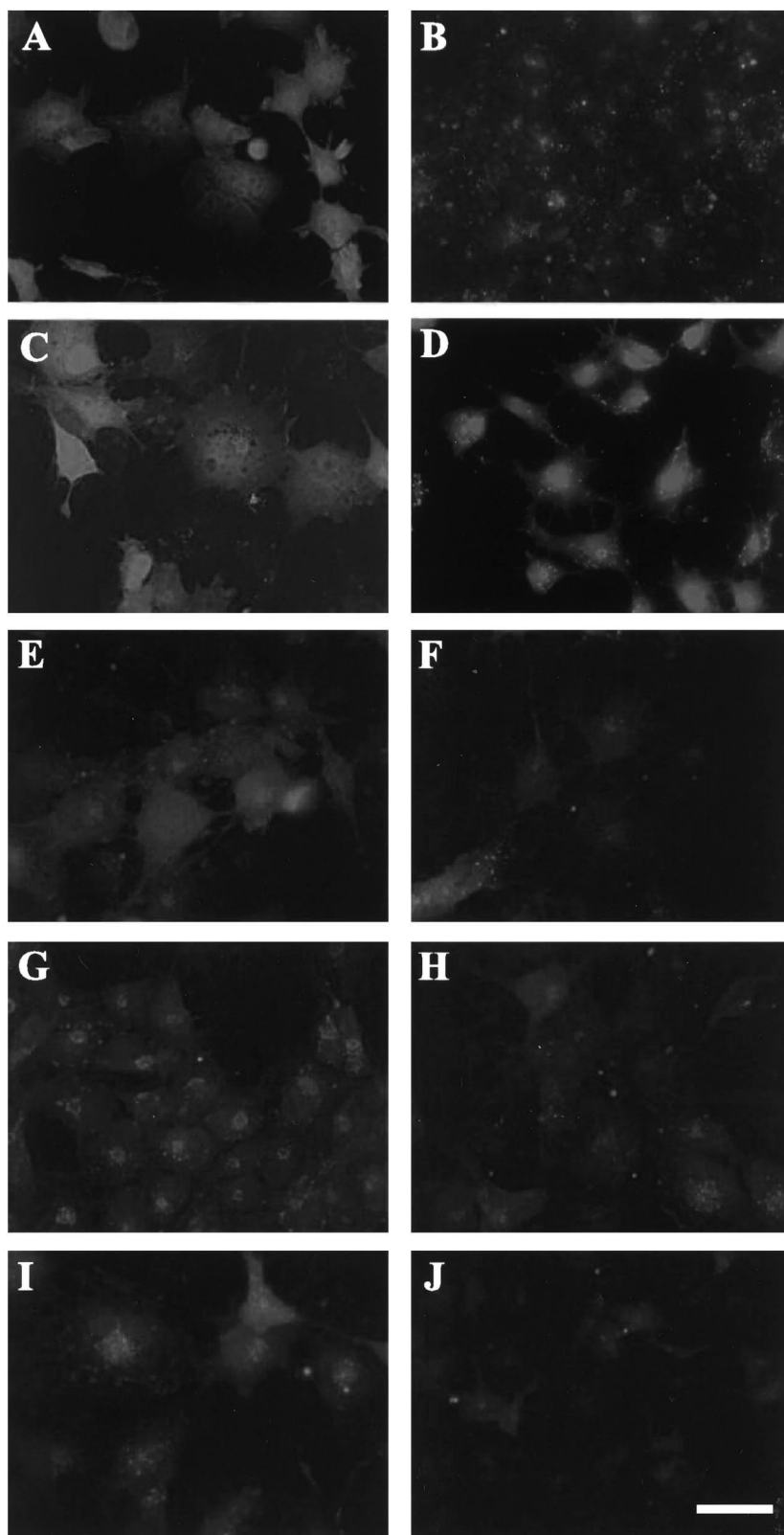


Fig. 3. Photomicrographs illustrating the production of NO in COS-1 cells reacted with DAF-2 DA. Under control conditions, there is basal NO production (A). Fixation with 4% PA or glutaraldehyde changed the pattern of fluorescence signal compared to cells without fixation (B). Sample images of treatment with 0.1 mM (C,E,G,I) or 1 mM (D,F,H,J) of the appropriate drug. Addition of a NO donor, SNP, increased the fluorescence intensity in a concentration-dependent manner (C,D). Cells treated with the NOS inhibitors NPA (E,F) or 1400W (G,H) presented reduced intensity of the NO fluorescent signal. The NO scavenger, PTIO, decreased NO fluorescent signal in a concentration-dependent manner (I,J). Scale bar = 25  $\mu$ m.

for the NADPH-d staining. Under basal, non-stimulated conditions, COS-1 and N2A cells express NOS-I and NOS-II, while SN56 cells only express NOSI. Moreover, no induction of NOS-II was observed either after treatment with NGF of SN56 cells for 24 h (data not shown).

Furthermore, colocalization of NO production (see below) with the NOS enzyme was assessed by combining the DAF-2 fluorescence with immunocytochemistry for each NOS subtype. As expected, all NO producing cells were NOS immunopositive (data not shown).

No significant signal was observed when the immunocytochemistry was performed in the absence of the primary antibodies (Fig. 1I).

### 3.3. Western blots

The immunocytochemistry results were confirmed by Western-blot analysis. NOS-I immunoreactivity was observed in all three of the cell lines as 160 kDa bands (Fig. 2, lanes 2–4). In contrast, NOS-II immunoreactivity was only observed in COS-1 and N2A cells as 130 kDa bands (Fig. 2, lanes 6–8), and no signal was detected in SN56 cells. The 160 and 130 kDa bands were in agreement with values reported for the NOS-I and NOS-II enzymatic subtypes, respectively. Moreover, similar bands were obtained in samples of brain tissue from rats injected with interleukin-1 $\beta$  a treatment that induces the expression of NOS-II [9]. On the other hand, NOS-III was not detectable in any of the three cell lines (Fig. 2, example of COS-1 cells is shown in lane 9), using a NOS-III antibody under conditions that detect this enzyme subtype in a positive lysate control derived from an aortic endothelium cell line.

### 3.4. Effect of incident light

The intensity of the fluorescent signal increased

proportionally to the amount of time that cells were stimulated with incident light (Fig. 5). Continuous exposure with epiluminescent light produced a faster increase in fluorescent signal as compared to the signal obtained by exposing the cells every 15 s to short intervals of light. This effect was directly proportional to the magnification power of the objective utilized for inspection. A  $\times 63$  magnification objec-

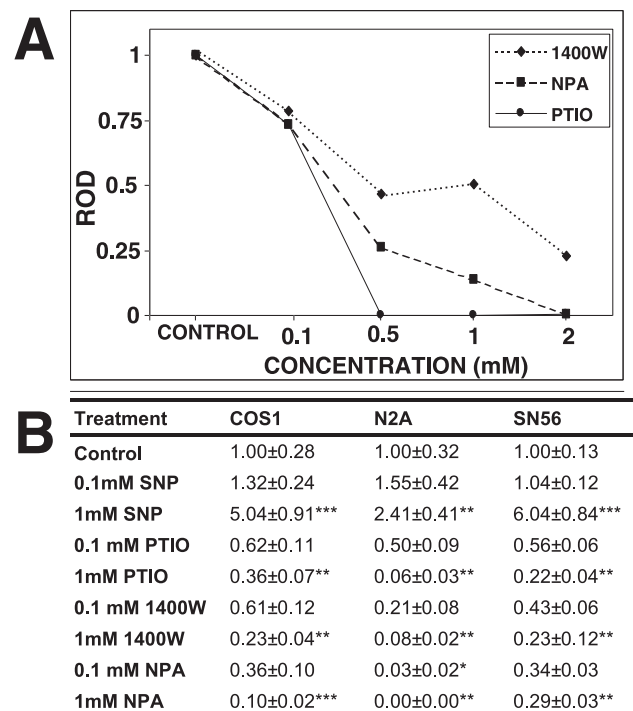


Fig. 4. (A) Effect of increasing concentrations of the NO scavenger, PTIO, and the NOS inhibitors NPA and 1400W on NO production in COS-1 cells. The results are expressed as relative optical densities (ROD). (B) Table showing the densitometric analysis of NO production in COS-1, N2A and SN56 cells by the DAF-2 method. One-way ANOVA followed by a Dunnett's post hoc analysis revealed a significant reduction of NO production with the NO scavenger and the NOS inhibitors compared to control cells. A significant increase was observed with the NO donor SNP (\* $P < 0.05$ ; \*\* $P < 0.01$ ; \*\*\* $P < 0.001$ ).

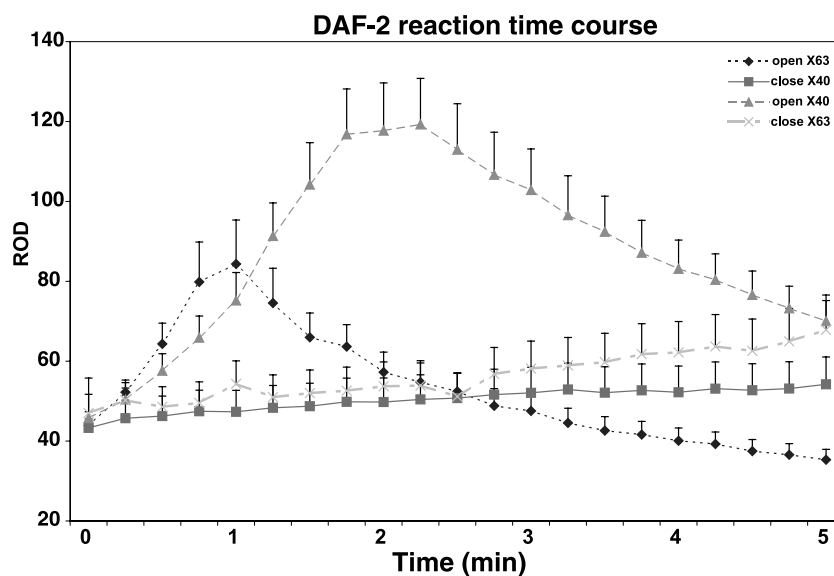


Fig. 5. Graph showing the time course of the intensity of the fluorescent signal of cells exposed to constant incident light (open), and under intermittent exposure with digitization every 20 seconds (close). In the same graph we show the effect of using a high (63 $\times$ ) and a lower (40 $\times$ ) power objective. Data are expressed as the mean ROD  $\pm$  S.E.M.

tive produced a faster increase in signal compared to a  $\times 40$  magnification objective. This increase was not synchronized in all cells examined, as some cells were peaking earlier than others, suggesting differences in metabolic activity. A plateau in fluorescence was reached as light stimulation continued and was followed by decay probably due to quenching.

### 3.5. Non-treated controls

Following incubation with the DAF-2 DA, we observed green-fluorescent signal in COS-1, SN56 and N2A cells, that corresponded to basal NO production (Fig. 3A).

In general, we observed a heterogeneous distribution of the green fluorescent signal within, and between cells. In COS-1 cells, a low signal was observed that resembled the cytoskeleton. In addition, a more intense punctated pattern was observed, which was localized in the cytoplasm of the soma and in differentiated fiber-like structures. The overall distribution was similar to that observed with immunocytochemistry of NOS and NADPH-d activity, confirming that NO is the result of the NOS activity. In contrast, and likely due to NO diffusion, cell nuclei were positively stained. The pattern of fluorescence intensity observed among SN56 and N2A cells was

also heterogeneous, probably reflecting the differential metabolic stages of the cells. Because of the round shape and relatively large nuclear size, the subcellular pattern of DAF-2 fluorescence in these cell lines was less striking than in COS-1 cells. The fluorescence signal was almost undetectable in control cells incubated without DAF-2 DA.

### 3.6. NO donor

Incubation of cells with the NO donor SNP (0.1 and 1 mM) induced a significant increase in fluorescent intensity (Figs. 3C,D and 4B). The effect was most significant at a concentration of 1 mM.

### 3.7. NOS inhibitors

Incubation of COS-1 cells with increasing concentrations (0.1, 0.5, 1 and 2 mM) of the NOS inhibitors 1400W (Fig. 3E,F) and NPA (Fig. 3G,H) resulted in a concentration-dependent decrease in fluorescent intensity (Fig. 4A). Both inhibitors produced their maximum effect at a concentration of 2 mM. Based on these results, we selected two subsaturating doses (0.1 and 1 mM) to compare the response of the other cell lines to the NOS inhibitors and observed the same dose-dependent inhibitory effect (Fig. 4B).



### 3.8. NO scavenger

To assess that the fluorescence signal was the result of NO production, we incubated the COS-1 cells in media containing increasing concentrations the NO scavenger PTIO (0.1, 0.5, 1 and 2 mM). Similar to effects of the NOS inhibitors, the fluorescence signal decreased in a dose-dependent manner with PTIO (Figs. 3I,J and 4A). At 1 mM PTIO the fluorescence signal was significantly reduced. The same pattern of results was observed in N2A and SN56 cells (Fig. 4B).

### 3.9. Effect of fixation

We studied the effect of fixation in cells reacted with DAF-2. We observed that a fixative containing a mixture of 0.2% glutaraldehyde and 4% paraformaldehyde (PA) abolished the DAF-2 fluorescence signal. Fixation with 4% PA produced a punctate fluorescence pattern (Fig. 3B), while 2% PA eliminated most of the signal in the periphery, leaving fluorescence in the center of the cell. Control cells reacted with DAF-2 that underwent no fixation presented a characteristic pattern of the fluorescent signal. Fixation abolished the changes in fluorescence signal observed in unfixed cells.

## 4. Discussion

In the present study, we show the *in situ* production and subcellular distribution of NO in three commonly used cell lines: N2A, SN56 and COS-1. The first two were chosen because of their neuronal characteristics [15,16], whereas COS-1 was used as a comparable non-neuronal cell line. First, the presence of the NO-synthesizing enzyme was indirectly confirmed by cytochemistry using the NADPH-diaphorase method. Second, we demonstrated the presence of NOS subtypes I and II in two of these cell lines, COS-1 and N2A, and the NOS subtype I in SN56 cells by immunocytochemistry and Western blots. Finally, we validated the DAF-2 method to study the *in vivo* cellular distribution and regulation of NO production, using NO donors and NOS-specific inhibitors to confirm that the fluorescent signal reflects NO levels. We also showed that the DAF-fluo-

rescence signal is affected by the conditions of cell fixation and of incident light.

The NADPH-diaphoretic activity was first used as a potential marker of NOS in COS-1, SN56 and N2A cells. Our results are consistent with those previously observed in N2A cells [17]; however, this is the first report of the presence of NADPH-diaphoretic activity in COS-1 and SN56 cells. Because NADPH-d is also a marker for other diaphoretic enzymes, such as the cytochrome P450, we used specific antibodies to determine the presence and subtypes of NOS. Our immunocytochemistry and Western blot results are consistent with the presence of NOS subtypes I and II in N2A and COS-1 cells, and only subtype I in SN56 cells. Interestingly, although the presence of NOS-I in N2A cells has been previously reported [17], the authors did not observe the NOS-II isoform in their study. Presently, we have no explanation for this discrepancy other than different culture conditions or differentiation stages of the cultured cells.

The expression of the inducible isoform of NOS (NOS-II) under non-stimulated conditions in COS-1 and N2A cells represents a novel and unexpected finding. Although NOS-II has been described in many cell types, its expression always followed induction by immunologic or inflammatory stimuli (see [8] for a review), or by growth factors in the case of early stages of differentiating neurons (see [18] for a review). In our hands, the neuronal and the kidney cell lines, both expressed NOS-II when maintained under standard culture conditions in regular media supplemented with 10% FCS and without any further treatment.

The expression of a NOS protein was previously described in SN56 cells [19]. However, the subtype characterization was not possible because the antibody used recognizes a protein region common to all the isoforms [20,21]. Thus, to our knowledge, this is the first clear demonstration of expression of the neuronal isoform (NOS-I) in the cholinergic model. Nevertheless, we did not observe NOS-II expression in SN56 cells under standard culture conditions and these neurons lacked NOS-II induction even after treatment with NGF, a growth factor that leads PC12 cells to differentiation and NOS-II expression [22].

The present paper provides further evidence for

the utility of the DAF-2 system for the semiquantitative analysis and visualization of the subcellular production of NO in living cells. Although the specificity and detection limits of the DAF-2 system have been a subject of discussion, Kojima and collaborators [7] have demonstrated that the DAF-2 DA is a highly specific probe that does not recognize other reactive species such as  $O_2^{\cdot -}$ ,  $H_2O_2$ ,  $NO_2^-$  and  $NO_3^-$ . Besides, the low detection limits of DAF-2 (2–5 nM) make it an ideal method for detecting basal NO production in living cells. Thus, the combination of specificity and low detection limit of the DAF-2 DA technique offers great advantage when compared to other methods such as spin trapping or electrodes, that do not provide the subcellular anatomical resolution.

In our cell lines NO production was observed as a dispersed or punctate fluorescent signal in the cytoplasm. We have recently demonstrated that part of the punctate signal observed in COS-1 and PC12 cells is produced within mitochondria, a key metabolic organelle [23]. A similar fluorescent pattern has also been reported in brain slices [24]. Moreover, our results utilizing NOS modulators substantiate that the DAF-2 method reflects the enzymatic production of NO *in vivo*. Thus, while in the presence of NOS inhibitors or of a NO scavenger we observed that DAF-2 fluorescence signal decreased in a dose-dependent manner, the addition of a NO donor caused an increase in the fluorescence signal. Nevertheless, our stimulation/inhibition results were comparable in all the cell types studied, confirming and giving further evidence of the presence and regulation of different subtypes of NOS.

It is worthy to note that although the fluorescence intensity was increased in a concentration-dependent manner concomitantly with the amount of NO in our *in vivo* experiments, fixation affects the intensity and distribution of the DAF-2 fluorescent signal. We showed that strong fixation considerably reduce the NO fluorescent signal, resulting in an artifactual and punctate pattern, whereas under mild fixation only NO fluorescent signal in the periphery of cells is lost. This susceptibility to fixation seems to be in agreement with previous observations on the differential effect of fixation on NOS detection by immunohistochemistry and histochemistry, and NO detection by the DAF-2 method [25,26]. Other significant

factors affecting the fluoresce emission are the specimen illumination time and intensity, as recently reported by Broillet and collaborators [27]. We observed that, upon a variable and relatively short lag phase, emission increased gradually, reaching plateau values after 1–2 min and finally decaying. However, optimal conditions of constant exposure time and microscopic magnification allowed us to compare the effect of NO donors, inhibitors and scavengers in a semi-quantitative way. Broillet and collaborators also found that the NO detection by DAF-2 is enhanced by the presence of divalent cations, an important factor to be considered especially because of the changing  $Ca^{2+}$  concentration within the cell. Although cellular  $Ca^{2+}$  levels were not controlled in this report, it is suggestive that a series of treatments modulating NO at different levels mostly changed signal intensity, not distribution. Thus, under the described experimental conditions, our measurements would indicate changes in NO, rather than  $Ca^{2+}$ , levels. As we previously discussed [11], the use of the DAF-2 DA method in living cells requires very careful planning of the experimental conditions but it could be used as a semi-quantitative method to compare cells exposure to different treatments.

It is important to note that the cell lines used in this work have been used in a variety of studies without considering the possibility of endogenous production of NO. For example, transfection studies have been used as an *in vivo* model of gene expression and regulation [28–30]. More specifically, COS-1 and N2A cells have been used to express novel NOS clones [31–34] or to demonstrate the interaction with intracellular pathways such as cGMP activation [15]. Therefore, our finding of basal expression of NOS subtypes and NO production has a direct impact on studies using the cell lines herein described.

In conclusion, the present study demonstrates the presence of NOS protein and activity as well as the regulation of NO production in COS-1, SN56 and N2A cells. In particular, we provide cytological evidence for the subcellular distribution of NO and its synthesizing enzyme. Given the multiple physiological and pathological effects of NO in cell signal transduction pathways, our data is relevant for the interpretation of results of previous and future studies utilizing these cell lines.

## Acknowledgements

The authors acknowledge technical support from Sharon Burke and Linda H. Gates. This project was supported by NIMH Program Project (MH42251) and The Pritzker Depression Network.

## References

- [1] T.M. Dawson, V.L. Dawson, S.H. Snyder, Molecular mechanisms of nitric oxide actions in the brain, *Ann. N. Y. Acad. Sci.* 738 (1994) 76–85.
- [2] M.O. López-Figueroa, H.E. Day, H. Akil, S.J. Watson, Nitric oxide in the stress axis, *Histol. Histopathol.* 13 (1998) 1243–1252.
- [3] D.S. Bredt, S.H. Snyder, Nitric oxide, a novel neuronal messenger, *Neuron* 8 (1992) 3–11.
- [4] T.M. Dawson, D.S. Bredt, M. Fotuhi, P.M. Hwang, S.H. Snyder, Nitric oxide synthase and neuronal NADPH diaphorase are identical in brain and peripheral tissues, *Proc. Natl. Acad. Sci. USA* 88 (1991) 7797–7801.
- [5] B.T. Hope, G.J. Michael, K.M. Knigge, S.R. Vincent, Neuronal NADPH diaphorase is a nitric oxide synthase, *Proc. Natl. Acad. Sci. USA* 88 (1991) 2811–2814.
- [6] L.L. Moroz, R. Gillette, J.V. Sweedler, Single-cell analyses of nitroergic neurons in simple nervous systems, *J. Exp. Biol.* 202 (1999) 333–341.
- [7] H. Kojima, N. Nakatsubo, K. Kikuchi, S. Kawahara, Y. Kirino, H. Nagoshi, Y. Hirata, T. Nagano, Detection and imaging of nitric oxide with novel fluorescent indicators: diaminofluoresceins, *Anal. Chem.* 70 (1998) 2446–2453.
- [8] K.M. Rao, Molecular mechanisms regulating iNOS expression in various cell types, *J. Toxicol. Environ. Health B Crit. Rev.* 3 (2000) 27–58.
- [9] M.O. López-Figueroa, H.E. Day, S. Lee, C. Rivier, H. Akil, S.J. Watson, Temporal and anatomical distribution of nitric oxide synthase mRNA expression and nitric oxide production during central nervous system inflammation, *Brain Res.* 852 (2000) 239–246.
- [10] T.M. McLeod, A.L. Lopez-Figueroa, M.O. Lopez-Figueroa, Nitric oxide, stress and depression, *Psychopharmacol. Bull.* 35 (2001) 24–41.
- [11] M.O. López-Figueroa, C.A. Caamaño, M.I. Morano, H. Akil, S.J. Watson, in: C.K. Sen, L. Packer (Eds.), *Methods in Enzymology*, Academic Press, New York, 2001 (in press).
- [12] M.O. López-Figueroa, J.P. Ravault, B. Cozzi, M. Moller, Innervation of the sheep pineal gland by nonsympathetic nerve fibers containing NADPH-diaphorase activity, *J. Histochem. Cytochem.* 45 (1997) 1121–1128.
- [13] J.P. Borg, M.O. Lopez-Figueroa, M. de Taddeo-Borg, D.E. Kroon, R.S. Turner, S.J. Watson, B. Margolis, Molecular analysis of the X11-mLin-2/CASK complex in brain, *J. Neurosci.* 19 (1999) 1307–1316.
- [14] U.K. Laemmli, Cleavage of structural proteins during the assembly of the head of bacteriophage T4, *Nature* 227 (1970) 680–685.
- [15] S. Chaki, T. Inagami, New signaling mechanism of angiotensin II in neuroblastoma neuro-2A cells: activation of soluble guanylyl cyclase via nitric oxide synthesis, *Mol. Pharmacol.* 43 (1993) 603–608.
- [16] W.A. Pedersen, M.A. Kloczewiak, J.K. Blusztajn, Amyloid beta-protein reduces acetylcholine synthesis in a cell line derived from cholinergic neurons of the basal forebrain, *Proc. Natl. Acad. Sci. USA* 93 (1996) 8068–8071.
- [17] H. Ovardia, H. Rosenmann, E. Shezen, M. Halimi, I. Ofran, R. Gabizon, Effect of scrapie infection on the activity of neuronal nitric-oxide synthase in brain and neuroblastoma cells, *J. Biol. Chem.* 271 (1996) 16856–16861.
- [18] M.T. Heneka, D.L. Feinstein, Expression and function of inducible nitric oxide synthase in neurons, *J. Neuroimmunol.* 114 (2001) 8–18.
- [19] D. Personett, U. Fass, K. Panickar, M. McKinney, Retinoic acid-mediated enhancement of the cholinergic/neuronal nitric oxide synthase phenotype of the medial septal SN56 clone: establishment of a nitric oxide-sensitive proapoptotic state, *J. Neurochem.* 74 (2000) 2412–2424.
- [20] J.E. Brenman, H. Xia, D.S. Chao, S.M. Black, D.S. Bredt, Regulation of neuronal nitric oxide synthase through alternative transcripts, *Dev. Neurosci.* 19 (1997) 224–231.
- [21] M.J. Eliasson, S. Blackshaw, M.J. Schell, S.H. Snyder, Neuronal nitric oxide synthase alternatively spliced forms: prominent functional localizations in the brain, *Proc. Natl. Acad. Sci. USA* 94 (1997) 3396–3401.
- [22] N. Peunova, G. Enikolopov, Nitric oxide triggers a switch to growth arrest during differentiation of neuronal cells, *Nature* 375 (1995) 68–73.
- [23] M.O. López-Figueroa, C. Caamaño, M.I. Morano, L.C. Ronn, H. Akil, S.J. Watson, Direct evidence of nitric oxide presence within mitochondria, *Biochem. Biophys. Res. Commun.* 272 (2000) 129–133.
- [24] L.A. Brown, B.J. Key, T.A. Lovick, Bio-imaging of nitric oxide-producing neurones in slices of rat brain using 4,5-diaminofluorescein, *J. Neurosci. Methods* 92 (1999) 101–110.
- [25] K. Sugimoto, S. Fujii, T. Takemasa, K. Yamashita, Detection of intracellular nitric oxide using a combination of aldehyde fixatives with 4,5-diaminofluorescein diacetate, *Histochem. Cell Biol.* 113 (2000) 341–347.
- [26] T. Gonzalez-Hernandez, M.A. Perez de la Cruz, B. Mantolan-Sarmiento, Histochemical and immunohistochemical detection of neurons that produce nitric oxide: effect of different fixative parameters and immunoreactivity against non-neuronal NOS antisera, *J. Histochem. Cytochem.* 44 (1996) 1399–1413.
- [27] M. Broillet, O. Randin, J. Chatton, Photoactivation and calcium sensitivity of the fluorescent NO indicator 4,5-diaminofluorescein (DAF-2): implications for cellular NO imaging, *FEBS Lett.* 491 (2001) 227–232.
- [28] C.A. Caamaño, M.I. Morano, F.C. Dalman, W.B. Pratt, H.

- Akil, A conserved proline in the hsp90 binding region of the glucocorticoid receptor is required for hsp90 heterocomplex stabilization and receptor signaling, *J. Biol. Chem.* 273 (1998) 20473–20480.
- [29] F. Meng, G.X. Xie, R.C. Thompson, A. Mansour, A. Goldstein, S.J. Watson, H. Akil, Cloning and pharmacological characterization of a rat kappa opioid receptor, *Proc. Natl. Acad. Sci. USA* 90 (1993) 9954–9958.
- [30] R.C. Thompson, A. Mansour, H. Akil, S.J. Watson, Cloning and pharmacological characterization of a rat mu opioid receptor, *Neuron* 11 (1993) 903–913.
- [31] H. Adachi, S. Iida, S. Oguchi, H. Ohshima, H. Suzuki, K. Nagasaki, H. Kawasaki, T. Sugimura, H. Esumi, Molecular cloning of a cDNA encoding an inducible calmodulin-dependent nitric-oxide synthase from rat liver and its expression in COS 1 cells, *Eur. J. Biochem.* 217 (1993) 37–43.
- [32] H. Fujisawa, T. Ogura, Y. Kurashima, T. Yokoyama, J. Yamashita, H. Esumi, Expression of two types of nitric oxide synthase mRNA in human neuroblastoma cell lines, *J. Neurochem.* 63 (1994) 140–145.
- [33] A. Hokari, M. Zeniya, H. Esumi, Cloning and functional expression of human inducible nitric oxide synthase (NOS) cDNA from a glioblastoma cell line A-172, *J. Biochem. (Tokyo)* 116 (1994) 575–581.
- [34] H. Ooboshi, Y. Chu, C.D. Rios, F.M. Faraci, B.L. Davidson, D.D. Heistad, Altered vascular function after adenovirus-mediated overexpression of endothelial nitric oxide synthase, *Am. J. Physiol.* 273 (1997) H265–H270.